Published in final edited form as:
Nano Lett. 2011 December 14; 11(12): 5213–5218. doi:10.1021/nl2025272.

Pump-Intensity- and Shell-Thickness-Dependent Evolution of Photoluminescence Blinking in Individual Core/Shell CdSe/CdS Nanocrystals

Anton V. Malko[1], **Young-Shin Park**[2,3], **Siddharth Sampat**[1], **Christophe Galland**[2,4], **Javier Vela**[3], **Yongfen Chen**[3], **Jennifer A. Hollingsworth**[3], **Victor I. Klimov**[2,4], and **Han Htoon**[2,3]

[1]Department of Physics, The University of Texas at Dallas, Richardson, TX 75080, USA

[2]Chemistry Division, Los Alamos National Laboratory, Los Alamos, New Mexico 87545, USA

[3]Center for Integrated Nanotechnologies, Los Alamos National Laboratory, Los Alamos, New Mexico 87545, USA

[4]Center for Advanced Solar Photophysics, Los Alamos National Laboratory, Los Alamos, New Mexico 87545, USA

Abstract

We report a systematic study of photoluminescence (PL) intensity and lifetime fluctuations in individual CdSe/CdS core/shell nanocrystal quantum dots (NQDs) as a function of shell thickness. We show that while at low pump intensities PL blinking in thin-shell (4–7 monolayers, MLs) NQDs can be described by random switching between two states of high (ON) and low (OFF) emissivities, it changes to the regime with a continuous distribution of ON intensity levels at high pump powers. A similar behavior is observed in samples with a medium shell thickness (10–12 MLs), without however, the PL intensity ever switching to a complete “OFF” state and maintaining ca. 30% emissivity (“gray” state). Further, our data indicate that highly stable, blinking-free PL of thick-shell (15–19 MLs) NQDs (“giant” or g-NQDs) is characterized by nearly perfect Poisson statistics, corresponding to a narrow, shot-noise limited PL intensity distribution. Interestingly, in this case the PL lifetime shortens with increasing pump power and the PL decay may deviate from mono-exponential. However, the PL intensity distribution remains shot-noise limited, indicating the absence of significant quantum yield fluctuations at a given pump power intensity during the experimental time window.

Nanocrystal quantum dots (NQDs) have been considered promising materials for applications ranging from bio-imaging[1] and light emitting diodes (LEDs)[2] to lasers[3] and single photon sources.[4] NQDs possess many unique characteristics that are beneficial to these applications: size-tunable emission colors, high intrinsic photoluminescence (PL) quantum yields (QYs), and solution processability. Despite these favorable properties, PL intermittency, commonly referred to as PL “blinking”[5], represents a serious impediment to applications that rely on single-dot emission. Initially, the PL blinking was explained in terms of random cycling of the NQD between two well-defined states of high- (ON) and low- (OFF) emissivities. These two states were attributed, respectively, to neutral and charged NQDs assuming that the charged dot was non-emissive (or only weakly emissive) due to highly efficient nonradiative Auger recombination.[6]

Corresponding authors’ anton.malko@utdallas.edu, htoon@lanl.gov, klimov@lanl.gov.

It was discovered that the probabilities (*P*) of ON and OFF sojourn times exhibit a power law distribution, $P(t) \sim t^{-\alpha}$, with α of ca. 1.5, where *t* is the duration of the ON or OFF events.[7] This power-law distribution of the ON/OFF times was initially explained in the framework of a two-state model. The distribution of the OFF times was regarded as the consequence of an exponential distribution of return rates (resulting from the variation in trap depths), while the ON times were governed by the dynamically varying rate of reneutralization.[7,8] However, later rigorous statistical analyses of PL time trajectories have revealed a very complex nature of the blinking process that cannot be described adequately by this simple ON/OFF two-state picture.[9] For example, to explain prolonged ON times, Verberk et al.[10] have introduced a three state model (two emissive and one dark state), in which the PL from the charged state is permitted when the charge is trapped away from the core of the NQD. The analysis of the photon counting statistics of blinking NQDs has also revealed intensity variations of the bright state indicating the existence of several ON levels.[11]

More pieces of evidence on the involvement of multiple emissive levels in PL fluctuations has been revealed by time-tagged, time-correlated, single-photon counting (TCSPC) measurements of NQDs under pulsed laser excitation.[12] The studies by Fisher *et al.* have shown that PL from single NQDs exhibit variations not only with regard to the intensity (*I*), but also the lifetime (τ).[12a] More recently, Zhang et al[12b] have demonstrated that while some NQDs show a relatively narrow distribution of PL intensities and lifetimes, others show broad, continuous distributions of *I* and τ, with high- (resp. low-) intensity emission events correlating with longer (resp. shorter) PL lifetimes. These findings have led to the conclusion that while PL fluctuations in some NQDs can be indeed described by a simple two-state picture, in other cases this picture is invalid and the assumption of a continuous distribution of ON levels is required to explain the observed variations in the PL intensities and lifetimes. Zhang et al. attributed these continuously distributed ON levels to different charge states, that are produced by trapping of long-lived photo-ionization-induced charges in a distribution of remote sites located away from the core of the NQDs (e.g. at the core-shell or shell-ligand interfaces). The random migration of these charges from one site to another could lead to variations in radiative and nonradiative recombination rates that, in turn, would result in the observed correlated variations of PL intensities and lifetimes.[12b] A similar correlated variation could also result from fluctuations in the number of those remotely trapped charges, as suggested by recent findings that more than one trapped charge might be necessary to explain low quantum yields and fast dynamics of the OFF state.[12c]

In parallel with the efforts towards a better understanding of PL fluctuations, many efforts have been undertaken to suppress PL blinking. Early attempts focused on reducing the density and accessibility of surface states via manipulating the ligand and/or solution environment of the NQDs.[13] These approaches, though, could only provide environment-dependent, temporary suppression of blinking, which has a limited practical utility. Recently, almost complete and permanent suppression of blinking has been achieved in several new types of NQDs that are modified at the level of their intrinsic structure.[14] One type of such structures is represented by core/shell NQDs in which a CdSe core is overcoated with an especially thick [>10 monolayers (MLs)] CdS shell. We dubbed these structures “giant” NQDs (g-NQDs) due to their relatively large sizes (diameters of 10 – 15 nm).[14a, 15] While our initial study using continuous-wave (*cw*) excitation with ~200 ms bin time revealed that some of the g-NQDs with an ultra-thick (19ML) CdS shell exhibited completely suppressed PL blinking, more recent single-photon counting study by Spinicelli *et al.*,[16] showed that the PL of the thinner-shell (~10 CdS MLs) g-NQDs exhibited random transitions between two emissive states (termed “bright” and “gray”) that were characterized by slow and fast PL decays, respectively.

The above overview indicates that a larger variety of blinking behaviors can be observed in colloidal nanocrystals. However, it is still largely unclear how this variability is linked to factors such as the details of the NQD structure (e.g., the shell thickness in core-shell nanocrystals), the regime of excitation (e.g., *cw* vs. pulsed), the excitation power, and the excitation wavelength. The purpose of this Letter is to use CdSe/CdS NQDs with an increasing shell thickness to elucidate the evolution in PL fluctuations during the transition from "standard blinking" (thin shells) to "blinking-free" (thick shells) behaviors. For each shell thickness, we also evaluate the effect of pump intensity on PL fluctuations. Specifically, we apply time-tagged, time-correlated single-photon counting (TCSPC) to study PL intensities, lifetimes and blinking in individual CdSe/CdS NQDs with the shell thickness varied from 4 to 19 MLs. For thin-shell (4 – 7 MLs) dots we observe that the increase of pump fluence changes PL blinking from a two-state ON/OFF behavior to a blinking regime with a variety of emissive (ON) levels characterized by a continuous distribution of PL intensities and lifetimes. For dots with medium (10 – 12 MLs) shell thicknesses, at the lowest pump power we observe a blinking-free behavior, which is characterized by a shot-noise-limited intensity distribution. As the fluence is increased, the PL starts to fluctuate between two distinct emissive states ("bright" and "grey" in the terminology of Ref. 16). At higher pump intensities PL fluctuations become typical of a continuum of emission levels without, though, ever switching to the OFF state. In the case of the thickest shells (15 – 19 MLs), blinking-free PL with a narrow distribution of intensities is observed for all pump fluencies. We also observe that the PL lifetime, while uniform across the intensity distribution, continuously decreases with increasing pump intensity. We argue that the observed reduction in the PL lifetime can be explained by the transition from emission due primarily to a neutral exciton at lower intensity to emission from a charged exciton (formed via photo-ionization) at high excitation intensities. At intermediate pump levels, the emission is due to interplay between these two states. Because of the suppression of Auger recombination in thick-shell dots, the PL quantum yield of the charged exciton does not differ significantly from that of the neutral exciton, which leads to stable, blinking-free PL even in the case of fluctuations in the charge state of the NQD.

In our experiments, we use CdSe/CdS core/shell NQDs synthesized via a modified successive ion layer deposition procedure described in Ref. [14a]. For single-dot spectroscopy, NQDs prepared in hexane are dispersed onto a quartz substrate with the density on the order of 0.01 per μm^2. The sample is mounted on a translation stage of an optical microscope and NQDs are excited at 405 nm with 50 ps pulses through a 60×, 0.7 NA objective lens, which is also used to collect PL. The pulse-to-pulse separation (>400 ns) is set to be much longer than the PL decay time in order to ensure complete relaxation of excitons between sequential laser pulses. The collected PL is sent to a Perkin-Elmer avalanche photodiode (SPCM AQR-14) through long-pass excitation/emission filters that reject scattered laser light. Single photon counting is performed using Becker & Hickl SPC-630 electronics. The overall system time resolution is 400 ps. In addition to recording PL intensity trajectories on a "macro" timescale (ms to minutes), the measurement system records arrival times for each photon with respect to the excitation laser pulse. In this way, photons are time-stamped on the "micro" timescale, which allows us to compile a PL decay curve for any particular macro-time window or any point of the intensity distribution function.[12a]

For the quantitative analysis of single-NQD PL intensity trajectories, we compare the measured PL intensity distributions with those for Poisson photon statistics. Specifically, for each trajectory, we calculate the Mandel Q parameter defined as $Q=\frac{(\langle n^2\rangle - \langle n\rangle^2)}{(n)} - 1$, where n represents the number of PL counts measured within the 20 ms time bin. Parameter Q equals to zero in the shot-noise limit, but is positive (and much greater than unity) for PL

trajectories in standard nanocrystals characterized by super-Poissonian statistics.[11b] We utilize the analysis of Q values instead of a more traditional power-law analysis of the ON/OFF sojourn time distributions because the ON/OFF threshold levels, that are critical for the accurate power-law analysis,[17] are impossible to determine in the case of nonblinking thick-shell g-NQDs. We also extract PL decay dynamics for several windows of the intensity distribution histogram to investigate the correlation between the PL intensity and lifetime variations.

In Figures 1, 2 and 3, we compare the pump-level dependent PL data for 3 NQDs that represent thin- (4 – 7 MLs), medium- (10 – 12 MLs) and thick- (>15 MLs) shell samples, respectively. Columns (A) and (B) of the figures show the PL time trajectories and histograms of the distribution of PL intensities (count rates), respectively. Each row of the figure corresponds to a certain pump intensity indicated in the cor responding panel in terms of the average NQD occupancy generated per excitation pulse, $\langle N \rangle$, which is calculated from the pump fluence using absorption cross-sections determined from the volume of the NQDs[18] (also provided in Supplemental Information in Ref. [24]). Column (C) displays representative PL dynamics extracted for the intensity ranges (i–iii) marked in column (B). For most cases, we extract PL lifetimes using single exponential fits to the data. For multi-exponential dynamics shown for low-intensity PL ranges in Figure 1, we plot single exponential fits to the initial component of the curves. In PL decays in Figure 3, we disregard the initial, very fast component, which has a multiexcitonic origin, as discussed below. The extracted PL lifetimes are plotted as a function of PL intensity on top of the histograms in column (B) with open circles.

Intensity distribution histograms of a thin-shell (4 MLs) NQD (Figure 1, column B) show two peaks that correspond to a weakly emitting OFF level, positioned clearly above the background noise[19] and the ON level, which exhibits a wider distribution of PL intensities. The average count rate (n, defined as the number of counts per bin) in the OFF state remains almost unchanged with increasing pump intensity. The distribution of the count rates in the ON state is near Poissonian at low pump levels ($\langle N \rangle < 0.3$) however, it broadens significantly at higher pump intensities and eventually becomes much wider than the Poisson distribution (shown in Figure 1B by solid black lines).

The increasing deviation of the measured intensity distribution from the Poisson statistics can also be clearly seen in the Q vs. $\langle N \rangle$ plot in Figure 4a (circles). As $\langle N \rangle$ is increased from 0.2 to 5, the Q value increases progressively from 0.9 to 100. At the low pump intensity ($\langle N \rangle = 0.1$), PL lifetimes extracted from the single-exponential fits of “microtime- tagged” traces, selected for a narrow range of PL intensities ($\Delta n = 3$) in the count-rate histogram, exhibit a step-wise growth (from ~5 to ~23 ns) as n is increased and the PL signal is scanned/swept from the OFF to the ON level (open circles in Figure 1B1). The behavior, however, is different at higher pump intensities, when τ continuously increases with increasing PL intensity. While at lower intensities PL lifetimes are multi-exponential, they become mono-exponential on the high-intensity end of the PL distribution for all pump fluencies.

Previously, variations of PL intensity detected in single-NQD measurements have been analyzed using either a model of discrete states[7,8] (e.g., a single ON and a single OFF level) or a continuum of states.[12] An important observation in our studies is that the NQD can exhibit *both* discrete- and continuous-state behaviors depending on pump intensity. Specifically, the data in Figure 1 indicate that in the case of low excitation levels, the PL intensity and lifetime fluctuations can be described by a simple two-state model, in which the NQD randomly switches between well-defined ON and OFF states, each of which emits a Poissonian stream of photons with shot-noise-limited fluctuations. On the other hand, as

the pump fluence is increased, the NQD emission experiences an increasing deviation from Poisson statistics, which indicates the transition to the regime of continuously distributed ON levels. This transition is likely a result of the increasing role of photo-charging at high pump intensities which can be facilitated, for example, by effects of Auger-assisted ionization.[20] In this picture, the mono-exponential decay observed for the highest PL counts in histograms in Figure 1B can be attributed to purely radiative recombination of single excitons. Specifically, the values of 25 – 30 ns derived from the high-count rate traces in Figure 1C (red lines) are in good agreement with the radiative lifetimes in standard CdSe NQDs measured in both ensemble[21] and single-dot studies.[12a] At the same time, the multi-exponential character of decays at intermediate count rates can either be attributed to a varying recombination rate due to migration of photoinduced charges from one trap site to the other as was proposed by Fischer *et al.*,[12a] or perhaps, to a quick switching between neutral and charged exciton states on the timescale much shorter than the bin size (20 ms). We would like to emphasize that while prior reports did suggest the existence of continuously distributed ON states[11b, 12b], the pump-intensity dependent evolution from a single ON state to a continuum of emitting states in the *same* dot has not been reported up to this moment.

A different behavior with regard to PL intensity and lifetime variations is observed in medium-shell (12 MLs) NQDs (Figure 2). At low pump power ($\langle N \rangle < 0.1$), most of these NQDs exhibit blinking-free emission with a near-Poissonian PL intensity distribution as illustrated in Figure 2 (A1 and B1). As expected for a Poissonian emitter, the PL dynamics are nearly uniform across the PL-count-rate histogram and are characterized by 100 – 150 ns single-exponential decays (Figure 2B1 and 2C1).[22] These low-pump-intensity results are indicative of blinking-free PL originating from a single emissive state.

However, the situation changes with increasing pump intensities when we observe the emergence of additional emission levels. Specifically, for $\langle N \rangle = 0.3$ (Figure 2A2 – 2C2), the count-rate distribution becomes double-Poissonian and the time of PL decay, which is close to single exponential, varies step-wise from ~40 ns to ~150 ns in going from the lower- to the higher-intensity peak in the PL count-rate histogram. These results point towards the existence of two emissive states. The high-count-rate state is the same as one observed at the lower pump level, as indicated by direct scaling of the average count rate (changes from ~10 to ~30) with $\langle N \rangle$ (changes from 0.1 to 0.3). The lower-count-rate state likely develops as a result of photo-charging and it corresponds to the situation of the increased nonradiative decay rate.

Two emitting states with similar characteristics were previously observed in g-NQDs by Spinicelli *et al.* and were explained in terms of neutral and charged excitons, with PL in the latter case being partially quenched by Auger recombination.[16] In standard NQDs, charged states (trions) are almost completely “dark” because the rates of Auger decay greatly exceed those of radiative recombination. On the other hand, as we demonstrated in Refs [23, 24], Auger decay is suppressed in g-NQDs, and therefore, trions can exhibit relatively large PL emission efficiencies (~19% according to Ref. 16). As a result, a charged exciton is transformed into a moderately emitting, “gray” state.

As in the case of data in Figure 1, the results of Figure 2 highlight a significant effect of pump intensity on the nature of emitting states in nanocrystals. When pump level is increased further (two upper sets of panels in Figure 2), we observe the emergence of a quasi-continuum of emissive levels. Specifically, the histograms of Figure 2B3 and 2B4 show a broad intensity distribution that could be described by a sum of five or even more simulated Poisson distributions. In accord with this observation, the plot of PL decay times vs. count rates (open circles in Figure 2B3 and 2B4) also shows a continuous increase in τ

with increasing PL count rate.[25] However, interestingly, we observe that the PL intensity distribution exhibits broadening with pump power only in the range of $\langle N \rangle \sim 0.1–1.0$, and gets narrower with a further increase of a pump fluence. This behavior can be seen more clearly in the Q vs. $\langle N \rangle$ plot (Figure 4a), which shows the saturation and even a slight decrease of Q when $\langle N \rangle$ becomes greater than 1.0 (squares). This narrowing of PL intensity distribution can be caused by the suppression of charge fluctuations that result from saturation of trap sites at higher pump levels. In contrast to this narrowing, the thin-shell (4 MLs) nanocrystals display a monotonous increase of the Q value, indicating the continuous broadening of PL intensity distribution with pump power. These findings lead to the conclusion that the spread of emissive levels contributing to PL in these CdSe/CdS NQDs decreases with increasing shell thickness.

Yet another behavior is observed in the case of the thickest-shell g-NQDs (15 – 19 MLs). A representative collection of data from a 19 ML g-NQD is displayed in Figure 3. Each of the intensity distribution histograms (column B of Figure 3) shows a single peak, which can be closely described by a Poisson distribution function. Figure 4 (triangles) also shows that for all pump intensities the Q values are relatively low, being in the range of 0.2 – 0.4. Accordingly, the PL decay dynamics are observed to be uniform across the distribution of the PL counts for any given pump power. At the lowest power of $\langle N \rangle = 0.25$, the decays are nearly single- exponential and correspond to emission from a single-exciton state. At higher pump fluencies, the dynamics becomes multi-exponential. However, we observed a wide variation in PL dynamics of blinking-free g-NQDs with some dots exhibiting double exponential decay even at the lowest pump power. The origin of fast initial component could be due to charged multiexcitons as discussed later or, due to plain biexciton contribution as observed and modeled for a subset of these dots (see Supplementary Information; Figure S1)

Although both PL intensity and lifetime fluctuations are completely suppressed at a fixed pump power, the slowest decay component of thick-shell g-NQDs accelerates with increasing excitation intensity. This point is illustrated in Figure 4b where we plot single-exciton decay constant τ_1 as a function of pump power for the g-NQDs from Figure 3 and Figure S1. This plot reveals that τ_1 decreases from ca. 75 ns (104 ns for the dot in Figure S1) to ca. 40 ns (60 ns) as the pump power is increased from $\langle N \rangle = 0.25$ to 7. This behavior is fully reversible; however, we often observed permanent signal degradation when much higher pump fluencies ($\langle N \rangle > 10$) were used. This observation indicates that although the changes in pump fluence do not alter the blinking-free character of PL of thick shell g-NQDs they do affect the recombination dynamics of the emissive state.

According to the popular charging model, the suppression of PL intensity and lifetime fluctuations observed in g-NQDs could result either from complete suppression of the random charging or suppression of the Auger process. In the first scenario the NQDs would be permanently locked in a charge-neutral state and the single-exciton lifetime would, therefore, remain unchanged with increasing pump fluence. Our observation of the increased PL decay rate at higher pump powers indicates that this is not the case, suggesting that the thick shell of our g-NQDs, while perhaps suppressing photo-charging at low fluences (as suggested in Ref. [24]), still does not completely inhibit photo-ionization, and hence, charge fluctuations at high excitation levels.

In the case of a fluctuating charge state, blinking-free PL is still possible if Auger recombination is considerably suppressed and, as a result, neutral and charged excitons have similar PL QYs. However, our recent study[24] reveals that while all of the thick shell g-NQDs produce fluctuation-free PL, their biexciton PL QYs vary widely from <0.2 to 0.9. This suggests that blinking-free emission is possible even in the presence of fairly efficient

Auger recombination. This seems to contradict to our assessment that photo-charging is *not* completely inhibited in these structures, at least at high pump levels.

This apparent controversy can be reconciled if we take into account that Ref. [24] analyzed emission efficiencies of *biexcitons* while the process of photo-charging, which is likely responsible for observed shortening of PL lifetime in the present experiments, creates *trions*. It is feasible that in g-NQDs the Auger decay rates are different for *negative* (X^-) and *positive* (X^+) trions. For example, based on the difference in the degree of spatial confinement for holes (confined to the small volume of the CdSe core) and electrons (delocalized over the entire volume of a g-NQD) and a higher density of the valence-band states compared to the conduction-band states, one might expect a faster Auger decay for X^+ than X^-. The Auger decay of a biexciton can be thought of as occurring via two pathways involving both X^+ and X^- In the case of a faster decay of X^+ it will be dominated by the route involving the positive trion. Photo-ionization, on the other hand, can create primarily negative trions, and therefore, the rate of Auger decay in charged NQDs will be governed by X^- rates and be considerably slower that the biexciton decay rate. Further, due to enhanced radiative decay, the PL quantum yield of the negative trion can be comparable to that of a neutral exciton. Therefore, fluctuations between the neutral and negatively charged excitons may occur *without* causing significant fluctuations in the PL intensity and result in apparent blinking-free PL emission. At intermediate pump levels, these charge fluctuations can lead to multi-exponential PL dynamics; this is indeed observed in our samples.

Since the probability of photoinduced charging increases with pump fluence, the corresponding increase in the time spent by the dot in the charged state would lead to the observed acceleration of the PL decay. Indeed, under these conditions, the recombination of a negative trion should be twice faster than a neutral exciton. The fact that the ratio of PL lifetimes measured at low (dominated by neutral exciton decay) and high (dominated by X^-) excitation intensities is approximately two (Figure 4B) supports this scenario. The above explanation still requires careful verifications. Most direct way to confirm our hypothesis about different rates of Auger decay for X^+ and X^- in g-NQDs is through single-dot measurements of PL dynamics in the regime of controlled charging. These studies are currently in progress in our group.

To summarize, we observe that PL fluctuation behaviors of CdSe/CdS NQDs are strongly affected by both the excitation level and the shell thickness. While at the lowest pump intensity, for all shell thicknesses these NQDs emit from a single state, at higher pump intensities the number of emitting levels depends on shell thickness. Specifically, for thin-shell samples we observed a multitude of emissive levels as indicated by a wide distribution of PL intensities and large values of the Mandel parameter ($Q >> 1$). On the other hand, the high-fluence PL intensity distribution narrows down with increasing shell thickness until it converges to a nearly Poissonian profile ($Q < 1$) for the thickest, 19 ML-shell dots. Because the PL lifetime shows a continuous reduction with increasing pump power in this latter case, we propose that despite a blinking-free behavior, two different states (neutral and charged excitons) may participate to the PL with relative contributions defined by the time spent in each of these states. The apparent blinking-free PL behavior would result from suppressed Auger recombination of a charged exciton (trion), which can lead to the situation where the charged and neutral excitons have similar PL QYs. Because of the asymmetry between the conduction and valence bands in II–VI semiconductors and the difference in the degrees of spatial confinement for electrons and holes in our core/shell structures, the Auger decay rate of a positive trion may exceed that of the negative trion. Therefore, Auger decay of a biexciton (contributed by both X^- - and X^+-like channels) can be faster than that of a negative trion. This could explain a coexistence of a fairly efficient Auger decay of a biexciton with blinking-free PL as previously observed for some of the g-NQDs.[24]

Supplementary Material

Refer to Web version on PubMed Central for supplementary material.

Acknowledgments

This work was conducted, in part, at the Center for Integrated Nanotechnologies (CINT), a U.S. Department of Energy, Office of Basic Energy Sciences (OBES) user facility. Work of A.V.M. was supported by UT Dallas start-up funds. Y.P. is supported by CINT. Y.G., J.V., Y.C. acknowledge Los Alamos National Laboratory Directed Research and Development Funds. V.I.K. is supported by the Chemical Sciences, Bioscience and Geosciences Division, OBES, Office of Science (OS), U.S. DOE, J.A.H. acknowledges NIH-NIGMS Grant 1R01GM084702-01 and H.H. acknowledges a Single-Investigator Small-Group Research Award (2009LANL1096), OBES, OS, U.S. DOE.

References

1. Bruchez MP, et al. Science. 1998; 281:2013. [PubMed: 9748157]
2. (a) Colvin VL, et al. Nature. 1994; 370:354–357.(b) Caruge JM, et al. Nature Photonics. 2008; 2:247–250.
3. Klimov VI, et al. Science. 2000; 290:314. [PubMed: 11030645]
4. (a) Michler P, et al. Nature. 2000; 406:968. [PubMed: 10984045] (b) Lounis B, et al. Chem. Phys. Lett. 2000; 329:399.
5. Nirmal M, et al. Nature. 1996; 83:802.
6. Efros AL, Rosen M. Phys. Rev. Lett. 1997; 78:1110.
7. Kuno M, et al. J. Chem. Phys. 2001; 115:1028.
8. Shimizu KT, et al. Phys. Rev. B. 2001; 63 205316.
9. (a) Peterson JJ, Nesbitt DJ. Nano Lett. 2009; 9(1):338–345. [PubMed: 19072721] (b) Stefani FD, et al. Physics Today. 2009; 62:34–39. [PubMed: 20523758]
10. Verberk R, et al. Phys. Rev. B. 2002; 66 233202.
11. (a) Jung Y, et al. Chem. Phys. 2002; 284:181.(b) Margolin G, et al. J. Phys. Chem. B. 2006; 110:19053. [PubMed: 16986903]
12. (a) Fisher BR, et al. J. Phys. Chem. B. 2004; 108:143.(b) Zhang K, et al. Nano Lett. 2006; 6:843. [PubMed: 16608295] (c) Zhao J, et al. Phys. Rev. Lett. 2010; 104 157403.
13. (a) Hohng S, Ha T. J. Am. Chem. Soc. 2004; 126:1324. [PubMed: 14759174] (b) He H, et al. Angew. Chem., Int. Ed. 2006; 45:7588.(c) Fomenko V, Nesbitt DJ. Nano Lett. 2008; 8:287. [PubMed: 18095736]
14. (a) Chen Y, et al. J. Am. Chem. Soc. 2008; 130:5026. [PubMed: 18355011] (b) Mahler B, et al. Nat. Mater. 2008; 7:659. [PubMed: 18568030] (c) Wang X, et al. Nature. 2009; 459:686–689. [PubMed: 19430463] (d) Osovsky R, et al. Phys. Rev. Lett. 2009; 102 197401.
15. Vela J, et al. J. Biophotonics. 2010; 3:706–717. [PubMed: 20626004]
16. Spinicelli P, et al. Phys. Rev. Lett. 2009; 102 136801.
17. (a) Crouch CH, et al. Nano Lett. 2010; 10:1692–1698. [PubMed: 20364845] (b) Frantsuzov PA, et al. Phys. Rev. Lett. 2009; 103 207402.
18. Klimov VI. J. Phys. Chem. B. 2000; 104:6112. 6112–6123.
19. Background noise of 2–3 counts/20 ms time bin is mainly contributed by the detector dark counts and autofluorescence of the quartz substrate.
20. Klimov VI, McBranch DW. Phys. Rev. B. 1997; 55:13173.
21. Crooker SA, et al. Appl. Phys. Lett. 2003; 82:2793.
22. This long decay time can be understood as the result of smaller e and h wavefunctions' overlap due to partial electron de-localization into the shell as described in Ref [23a]
23. (a) Garcia-Santamaria F, et al. Nano Lett. 2009; 9(10):3482. [PubMed: 19505082] (b) Garcia-Santamaria F, et al. Nano Lett. 2011; 11:687. [PubMed: 21207930]
24. Park YS, et al. Phys. Rev. Lett. 2011; 106 187401.

25. At very high pump power the decay dynamics become bi-exponential. The longest decay constant however still exhibit similar continuous variation.

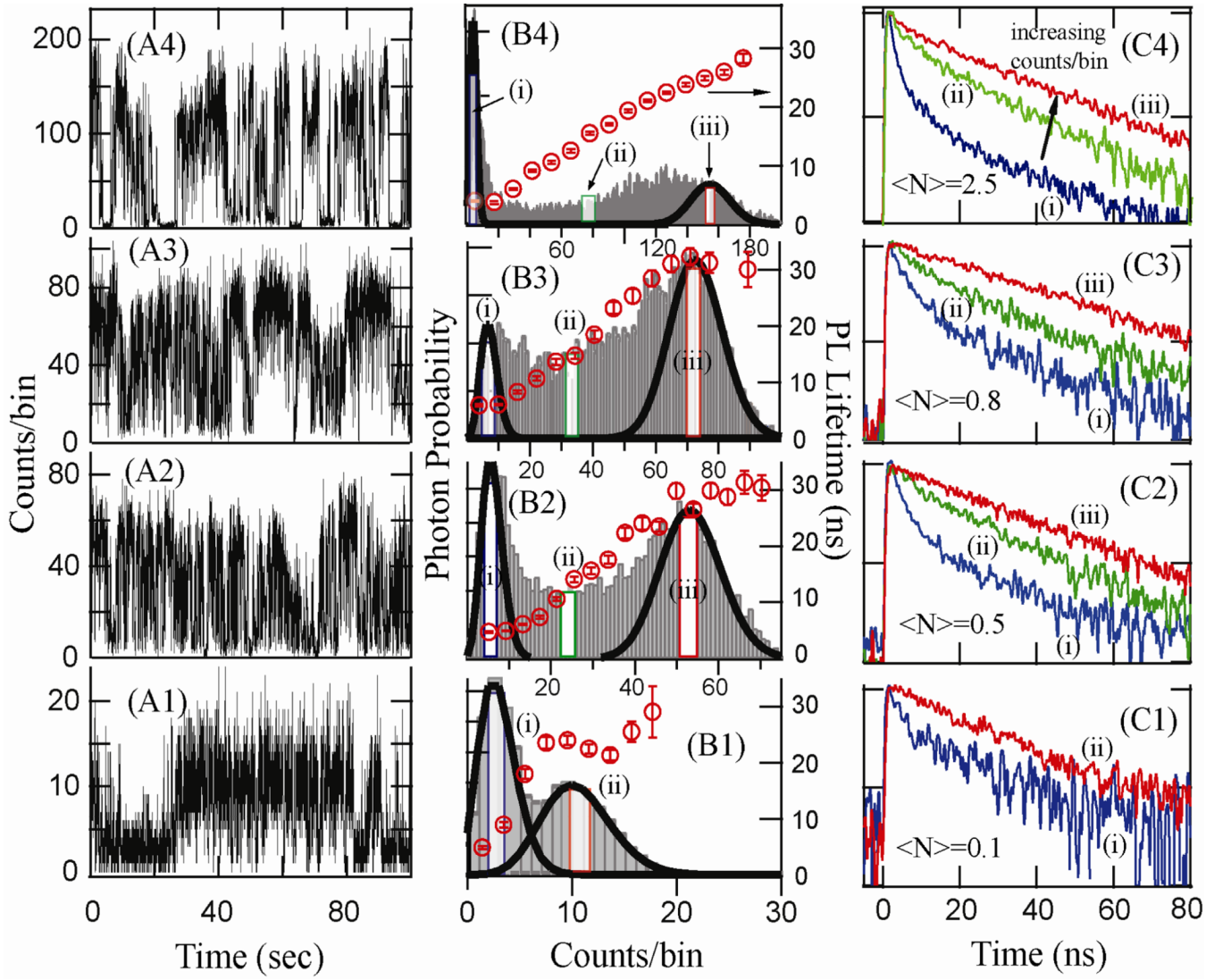

Figure 1.

A(1–4) PL emission intensity trajectories of a single CdSe/4CdS giant NQD as a function of the excitation power expressed in average number of e–h pairs per pulse ($\langle N \rangle$). B(1–4) Intensity histograms for each trajectory (shaded areas, left scale) and exciton PL lifetimes (open dots, right scale) for various intensities within the same trajectory. Black curves – Poissonian fits for an "OFF" state and for a highest "ON" state. C(1–4) PL emission lifetimes (log scale) corresponding to a particular intensity distribution (i)–(iii) within the histogram.

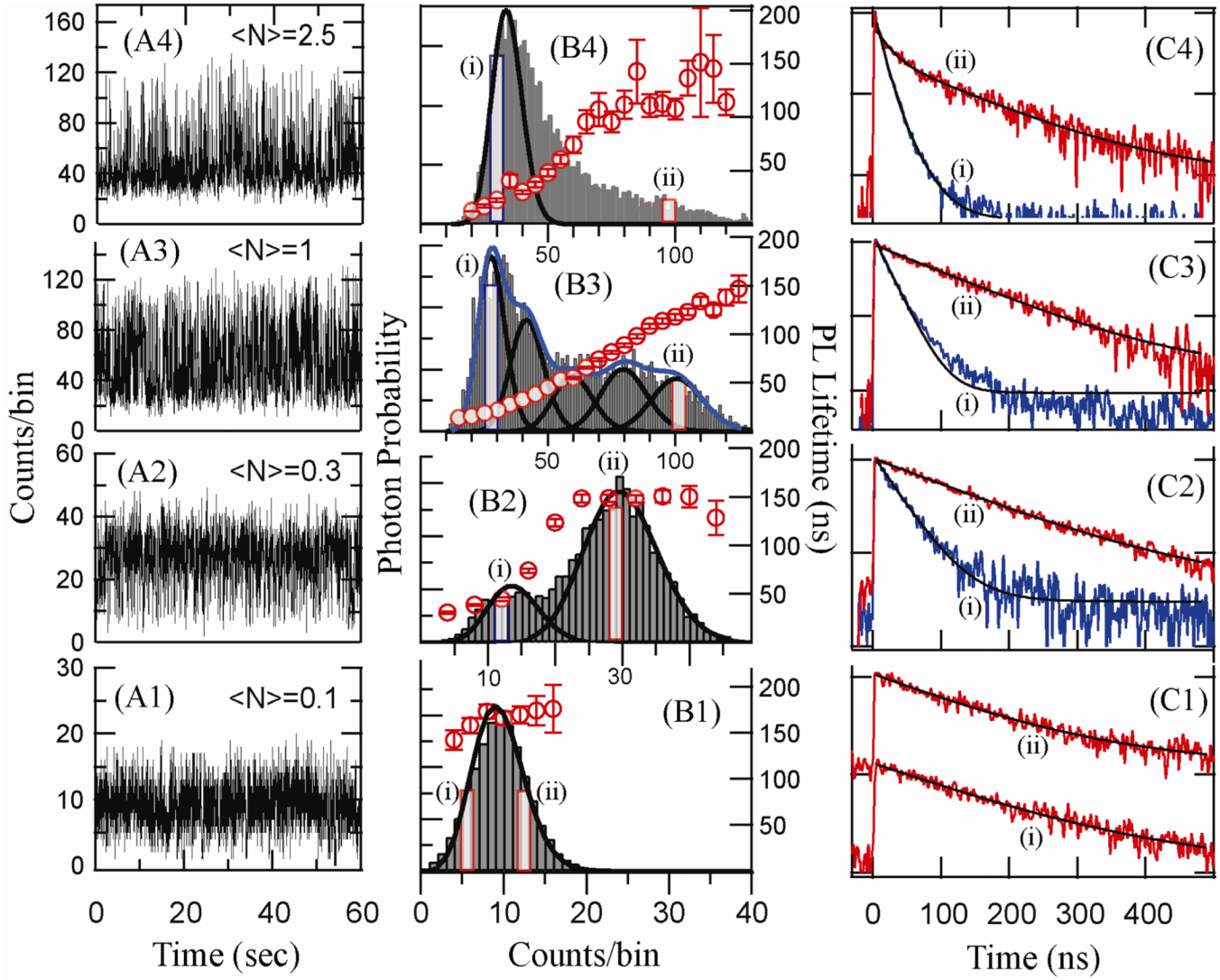

Figure 2.

A(1–4) Intensity trajectories for CdSe/12CdS dot. Trajectories show suppressed blinking and presence of the minimum intensity “grey” state. B(1–4) Intensity histograms for each trajectory (shaded areas, left scale) and exciton PL lifetimes (open dots, right scale) for various intensities within the same trajectory. C(1–4) PL emission lifetimes (log scale) at particular intensity distributions (i)–(ii) within each histogram. Black lines are single exponential fits on panels C(1–3), double exponential fit is used on panel C(4). Curves are offset for clarity on panel C(1).

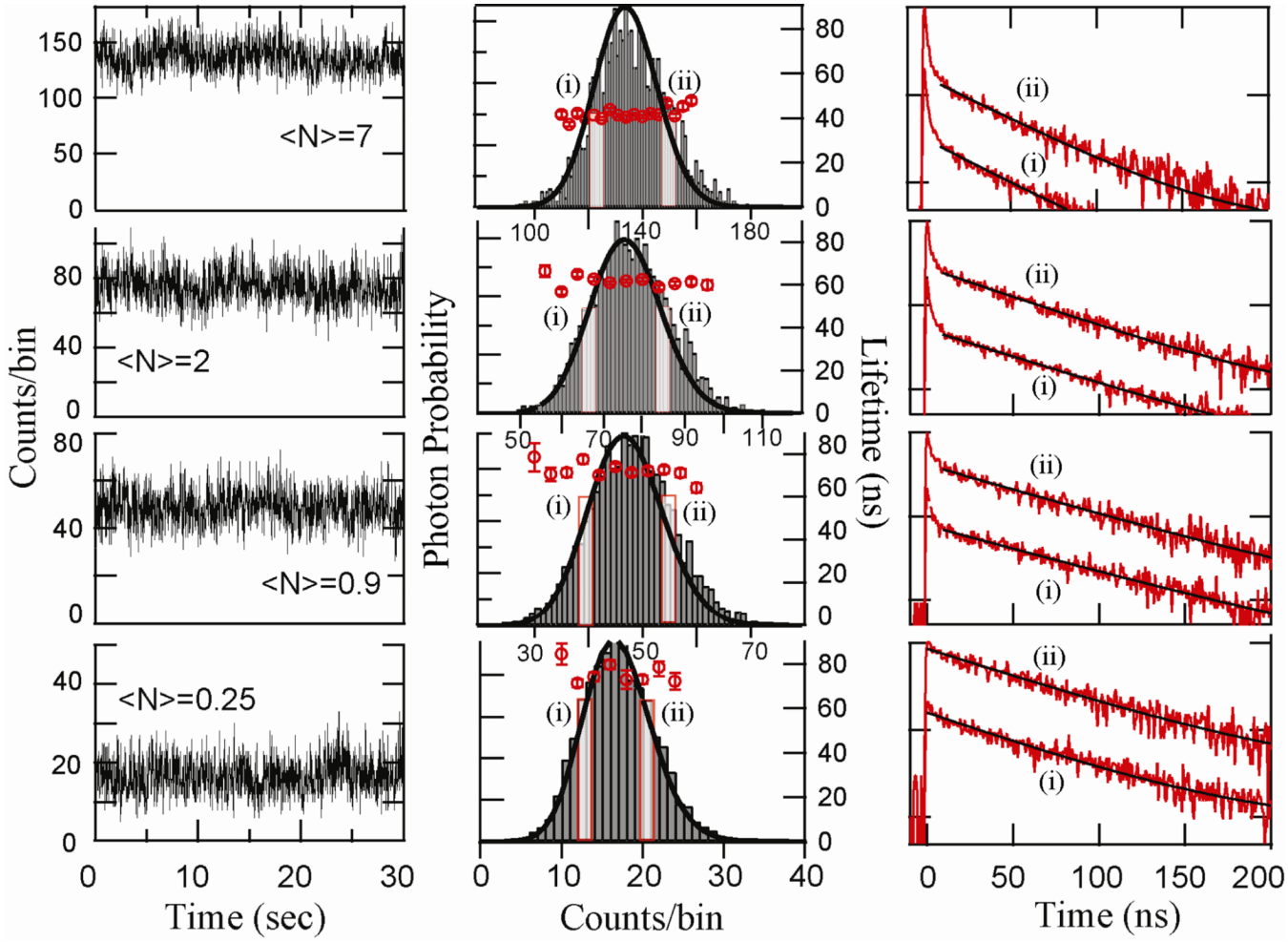

Figure 3.

A (1–4) Intensity trajectories for CdSe/19CdS dot. B (1–4) Intensity histograms showing the presence of a single emissive state at a given power and C(1–4) PL emission lifetimes extracted for two points at each distribution. Dashed black lines - single exponential fits to the slowest components of the decay.

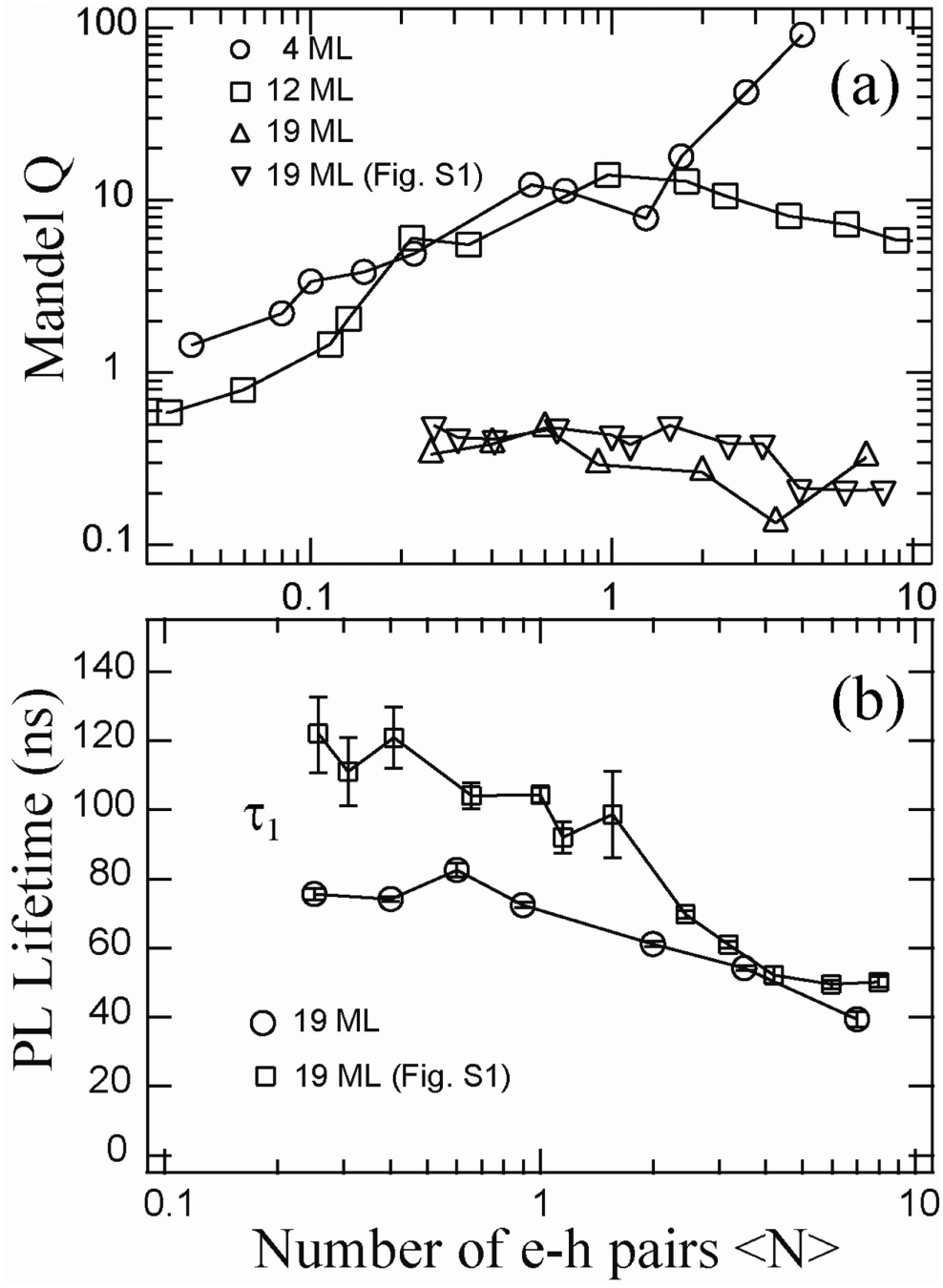

Figure 4.

(a) Mandel Q parameter vs. excitation level given in terms of $\langle N \rangle$ for 4 ML (circles), 12 ML (squares) and for 19 ML dots, one shown in Figure 3 and another in Suppl. Info Figure S1 (triangles). (b) Time constants (τ_1) for longest PL decay of 19 ML g-NQDs shown in Figure 3 and in Figure S1, plotted as the function $\langle N \rangle$. Solid lines – guide for the eye only.